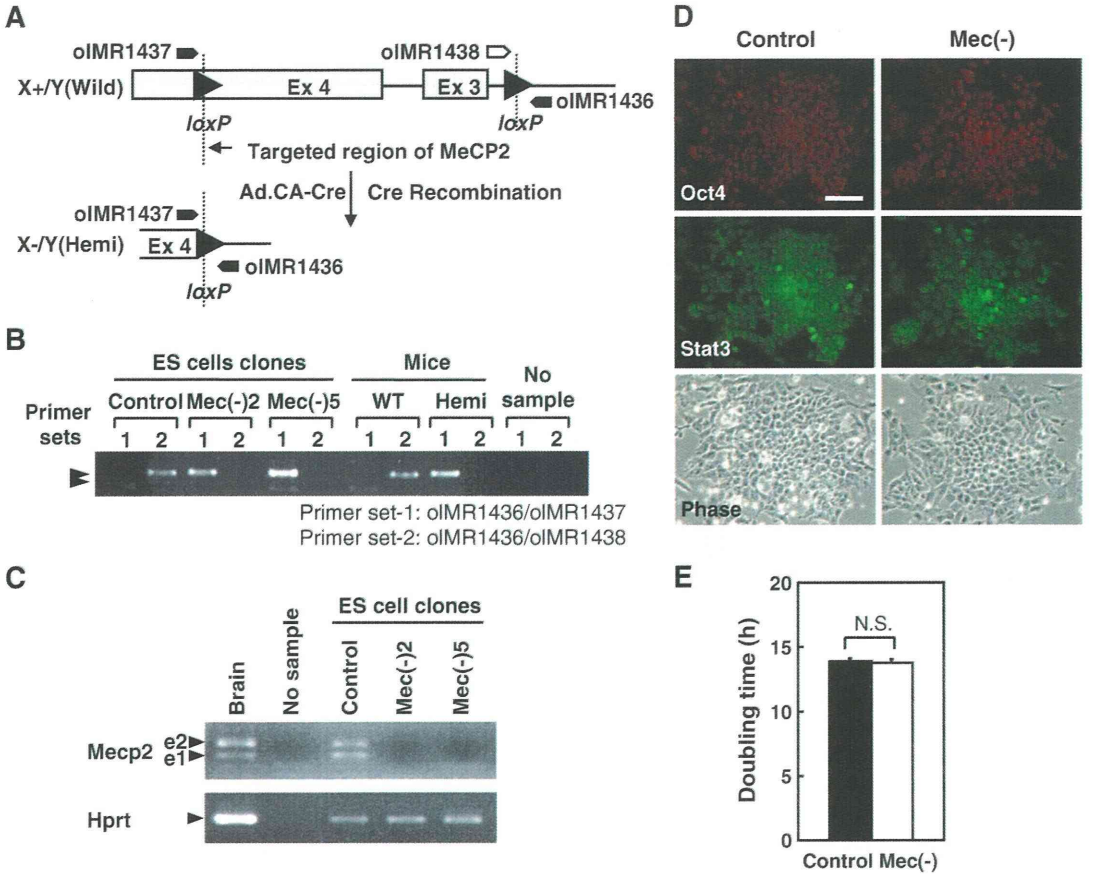

Fig. 1 – Generation and phenotypic analysis of MeCP2-null ES cells. (A) Targeted mutation of the Mecp2 locus. (B) Genotyping of control (Mecp2$^{+/y}$) and two MeCP2-null (Mecp2$^{-/y}$; Mec(–)) ES cell clones, and of MeCP2 wild-type and hemizygous mice was performed by PCR. Primer set 1 (oIMR 1437 and oIMR 1436) amplifies a ~400 bp mutant band, whereas primer set 2 (oIMR1438 and oIMR 1436) amplifies a 416 bp wild-type band. (C) mRNA expression of Mecp2 e1 and e2 variants in a control and two MeCP2-null ES cell clones was analyzed by RT-PCR. Wild-type mouse brain was used as a positive control. (D) The control and the MeCP2-null ES cells were stained with anti-Oct4 or anti-STAT3 antibody. Scale bar=80 μm. (E) Doubling times of undifferentiated control and MeCP2-null ES cells are shown. N.S., no significant difference (control versus MeCP2-null ES cells, n=19 each).

cells showed expression of both Mecp2 splice variants, e1 and e2, whereas neither Mecp2 variant was detectable in both Ad. Cre-infected MeCP2-null ES cell clones (Fig. 1C). Thus, two MeCP2-null (Mecp2$^{-/y}$) and one control (Mecp2$^{+/y}$) ES cell clones were efficiently generated. In the following experiments, we use one of two MeCP2-null ES cell lines (clone 2) and one control ES cell line.

2.2. *Loss of MeCP2 does not appear to affect undifferentiated ES cells*

We first examined whether MeCP2 is required in undifferentiated ES cells. Prominent expression of Oct4 and Stat3, markers of the undifferentiated state, was found in the nuclei of almost all cells in both MeCP2-null and control ES cells by immunostaining (Fig. 1D). No differences in undifferentiated growth were observed between the two (Fig. 1E). Thus, MeCP2 does not appear to be critical for maintaining the undifferentiated state or for ES cell growth.

2.3. *MeCP2 is not involved in the efficiency of neural differentiation*

RT-PCR analysis showed that both Mecp2 variants, e1 and e2, were expressed in control ES cells in the undifferentiated state, as well as throughout all developmental stages (Fig. 2A).

We examined the role of MeCP2 in neuronal differentiation by comparing the phenotypes of control and MeCP2-null ES cells during differentiation. Neither the number nor the morphology of the differentiating ES colonies was significantly different between the two groups, suggesting that MeCP2 is not essential for cell growth during neural differentiation (Fig. 2B and C).

We next examined whether MeCP2 affected neuronal differentiation by immunostaining for Nestin, β-Tubulin type III (TuJ), and Tyrosine hydroxylase (TH), markers for early neuronal cells (including NSCs), differentiated neurons, and DNs, respectively (Fig. 3A–C). The percentage of Nestin-, TuJ-, and TH-positive colonies reached a maximum on day

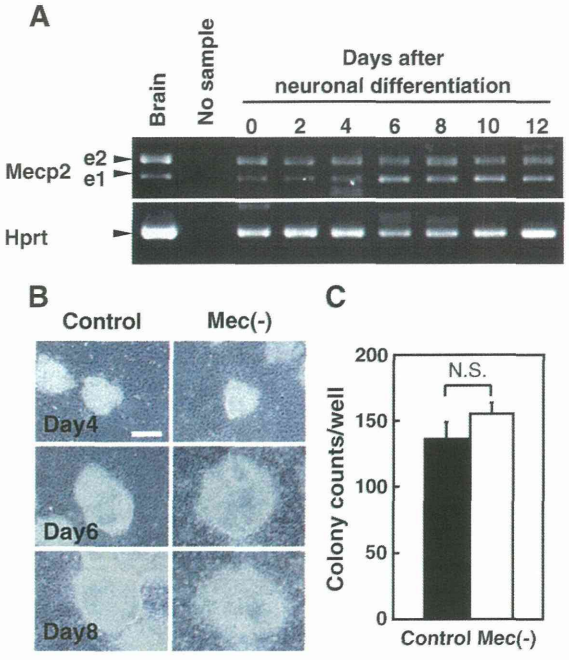

Fig. 2 – Neural differentiation of MeCP2-null ES cells. (A) mRNA expression of Mecp2 e1 and e2 variants in control ES cells on the indicated days after the start of co-culture on PA6 cells was analyzed by semi-quantitative RT-PCR. Wild-type mouse brain was used as a positive control. (B) Representative images of control and MeCP2-null ES cell colonies on the indicated days after co-culture on PA6 cells. Scale bar=200 μm. (C) The number of colonies per well was counted on day 10.

8 and did not differ between the two groups. Thus, loss of MeCP2 does not affect the efficiency of neuronal differentiation. The percentage of Nestin-, TuJ-, and TH-positive MeCP2-null colonies was higher than that of control colonies on day 4, and the percentage of Nestin-positive MeCP2-null colonies on day 12 was lower than that of the controls, although the slightly precocious differentiation was not significant. The results suggest that MeCP2 is not essential for induction of neuronal differentiation, at least induction toward DNs.

2.4. *Loss of MeCP2 causes immature resting and active membrane properties in ES cell-derived neurons*

To analyze neuronal maturity, the membrane properties of control and MeCP2-null ES cell-derived neurons were examined by electrophysiology on days 10–12 (Table 1). The peak current densities of the voltage-dependent Na^+ currents (I_{Na}s) underlying the rising phase of the action potential and the A-type K^+ currents (I_As) were significantly smaller in the MeCP2-null ES cell-derived neurons than in the controls (Fig. 4A and B). In contrast, the peak currents of the delayed rectifier K^+ currents (I_{DR}s) did not significantly differ between the control and MeCP2-null ES cell-derived neurons (Fig. 4C). In addition, the repetitive spikes showed a relatively high firing frequency and rundown in amplitude in the MeCP2-null ES cell-derived neurons (Fig. 4D). The rundown may be due to a decrease in expression of I_{Na}s and the I_As. These results suggest that MeCP2 contributes to the development of resting and active membrane properties, and that MeCP2-null ES cell-derived neurons do not reach maturity.

2.5. *MeCP2 does not appear to affect dopaminergic function*

To examine the involvement of MeCP2 in DN function, dopamine production and release were investigated by reverse phase HPLC in MeCP2-null and control ES cell-derived neurons on day 10 of culture. In response to a depolarizing stimulus, DNs derived from MeCP2-null ES cells released as much dopamine into the medium as did control cells (Fig. 5). Thus, MeCP2 is not critical for the dopaminergic function of DNs, at least in this experimental system.

2.6. *MeCP2 deficiency accelerates glial differentiation*

Because interactions between neurons and glia are essential for the development and function of neurons (Corbin et al., 2008; Stevens, 2008), we examined changes in expression of the glial marker GFAP in ES colonies during neural differentiation. GFAP-positive colonies emerged earlier and were present at a higher percentage on days 8 and 12 in MeCP2-null ES cells compared to controls (Fig. 6A and B), consistent with the GFAP expression observed in colonies (Fig. 6C). The significantly accelerated glial differentiation in MeCP2-deficient cells suggests that MeCP2 negatively regulates glial differentiation. In addition, the timing of differentiation, with the start of neuronal differentiation preceding the start of glial differentiation, as well as the presence of both neurons and glia in differentiated ES colonies mirror normal neural development (Qian et al., 2000; Stevens, 2008), underscore the usefulness of this experimental system.

3. Discussion

The overall role of MeCP2 throughout neural development, particularly at early stages before the onset of neural differentiation, has not been investigated due to the lack of a definitive experimental system or materials. In this study, we first demonstrated that MeCP2-null ES cell could be feasibly generated by applying the *in vitro* ACT method to loxP-floxed ES cells that were originally engineered for a generation of conditional knockout mouse (Takahashi et al., 2006). Just as there were no significant adverse effects from ACT on cell cycle regulation, cell viability, or the efficiency of differentiation in ES cells, the MeCP2-null and the control ES cells generated by ACT worked with no problems in several types of experiments in the previous and the present study (Takahashi et al., 2006). In addition, the co-culture method that was used in the present study has the advantages of both technical feasibility and high efficiency of dopaminergic differentiation (Kawasaki et al., 2000). Our experimental system of comparing MeCP2-null and control ES cells throughout their developmental stages, including in the undifferentiated state and at the early stage of neural development, provided important information about the role of MeCP2 in neural development.

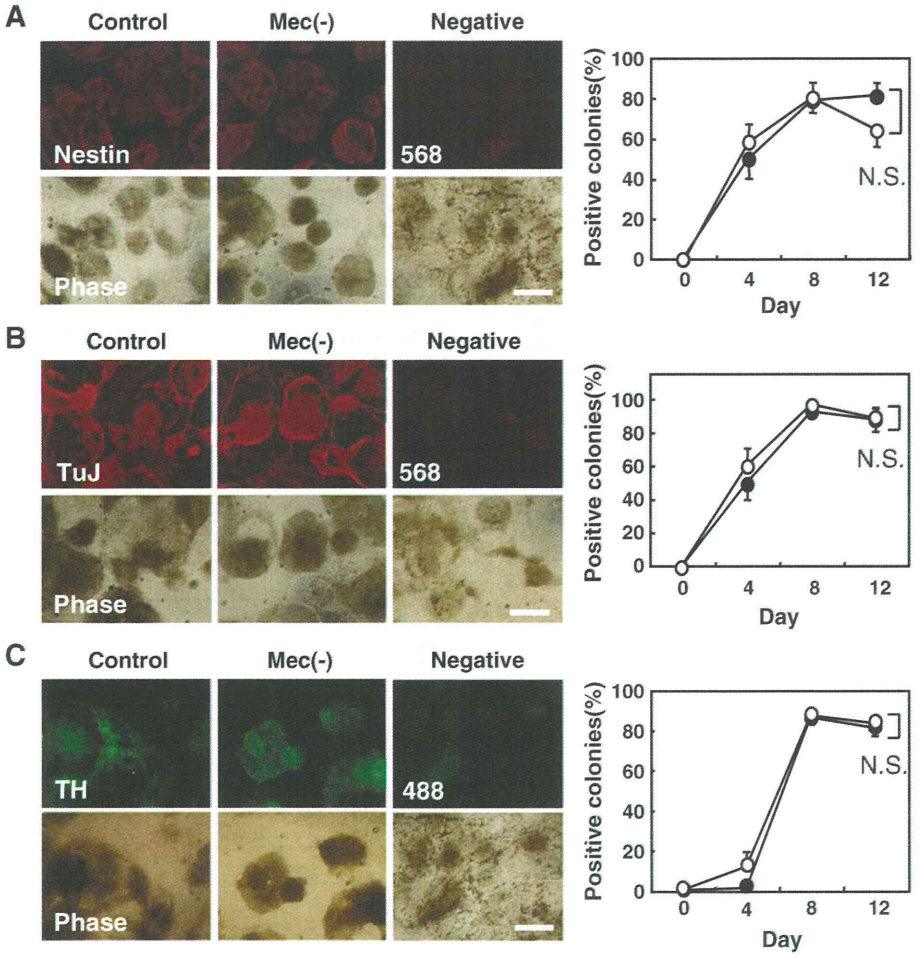

Fig. 3 – Neuronal differentiation of MeCP2-null ES cells. (A–C) Control (closed circle) and MeCP2-null (open circle) ES cells on days 4, 8, and 12 were stained with antibody against Nestin (A), TuJ (B), or TH (C). Negative control indicates colonies on day 12 that were stained with only the secondary Alexa Fluor 488 or 568 antibodies without primary antibodies. N.S., no significant difference (control versus MeCP2-null ES cells at each time point). Between 50 and 200 colonies per well were counted to calculate the mean ± SD (Nestin; $n=5$, TuJ; $n=5$, and TH; $n=3$) and the results were verified in three different experiments. Representative images from day 12 are shown on the left. Scale bar = 0.5 mm.

Using this system, we have clarified several important issues, some of which are consistent with previous findings. First, we demonstrated that MeCP2 is not essential for the maintenance or growth of undifferentiated ES cells, supporting the previous finding that absence of MeCP2 did not cause embryonic lethality in mice (Guy et al., 2001). Second, MeCP2 deficiency has a minimal effect on neurogenesis, consistent with the fact that the brains of RTT patients and MeCP2-null mice are morphologically and phenotypically normal at birth (Armstrong, 2002; Chahrour and Zoghbi, 2007). Thus, MeCP2 is likely not an essential part of the machinery that advances neurogenesis. On the other hand, while it has been reported that MeCP2 was involved in neuronal maturation rather than cell fate decisions (Kishi and Macklis, 2004; Smrt et al., 2007), the present results suggested that MeCP2 was remarkably somewhat involved in negative regulation of glial differentiation and neuronal maturation. Apparently inconsistent results between the previous and present studies may be due to the difference in experimental systems. For instance, MeCP2 was expressed in neurons and undifferentiated neuroepithelial cells at high and almost undetectable levels, respectively, in the experimental system of the previous study (Kishi and Macklis, 2004), whereas in the present system MeCP2 expressions were clearly detected in not only ES cell-derived differentiated neurons but also in undifferentiated ES cells. This aspect of the present experimental system may have the advantage of being able to sensitively and carefully detect any possible phenotypes in order to determine whether MeCP2 affects neural development, including gliogenesis, during any stage, including early stages before the onset of neural differentiation.

In contrast, MeCP2-null ES-derived neurons are electrophysiologically immature, suggesting that MeCP2 contributes to the development of the active membrane properties. Biella et al. have reported that voltage-gated Na^+ currents gradually increase during neuronal maturation, but that I_{DR}s is already

Table 1 – Differences in electrophysiological parameters between control and MeCP2-null ES-derived cells.

	Parameters	Control	Mec(–)
I_{Na}	Peak amplitude, pA	−1060±140(4)	−701.8±184.9(5)*
	Current density, pA/pF	−96.4±6.5(4)	−64.2±8.7(5)*
I_A	Peak amplitude, pA	89.0±32.2(4)	30.1±8.4(4)*
	Current density, pA/pF	8.3±1.7(4)	3.0±0.7(4)*
I_{DR}	Peak amplitude, pA	169.2±87.1(3)	105.7±53.4(4)
	Current density, pA/pF	15.8±7.2(3)	11.0±7.2(4)
	Membrane capacitance, pF	10.7±1.6(11)	10.3±1.8(13)
	V_{Rm}, mV	−52.8±11.4(6)	−52.1±10.7(7)
	Threshold, mV	−44.4±4.9(6)	−37.6±1.0(6)*
	Firing frequency, Hz	5.8±1.0(6)	9.3±0.8(6)*

I_{Na}; voltage-dependent Na^+ current, I_A; A-type K^+ current, I_{DR}; delayed rectifier K^+ current, V_{Rm}; resting membrane potential
Numbers in parentheses indicate the recording cell number.
Firing frequency is derived from mean firing rate during the injection of depolarizing current of which amplitude is two times of the threshold.
* Indicates statistical significance between the control and the MeCP2-null ES-derived neurons by Student's test with $p<0.05$.

at a mature state at early stages of neural development in ES-derived NSCs (Biella et al., 2007). The amplitude of I_As also increases during the late embryonic-early postnatal developmental period in hippocampal neurons (Ficker and Heinemann, 1992). Thus, MeCP2 may be required for neuronal maturation (development of voltage-gated Na^+ currents and I_As), suggesting that some neuronal symptoms in RTT may be caused by immature neuronal membrane properties.

In terms of the neural immaturity in MeCP2-deficient cultures, it should be noted that loss of MeCP2 led to drastically increased gliogenesis. The involvement of MeCP2 in gliogenesis may be supported by previous studies, although their data were indirect and limited to middle and late phases of neural development (Deguchi et al., 2000; Nagai et al., 2005; Setoguchi et al., 2006). For instance, inhibition of MeCP2 in E18 non-neuronal mouse cells inhibited cell growth (Nagai et al., 2005), and ectopic overexpression of MeCP2 inhibited E14.5 neuroepithelial cells from differentiating into GFAP-positive cells (Setoguchi et al., 2006). Moreover, MeCP2 binds to a highly methylated region in the GFAP promoter. Thus, the authors suggested that MeCP2 is involved in restricting differentiation

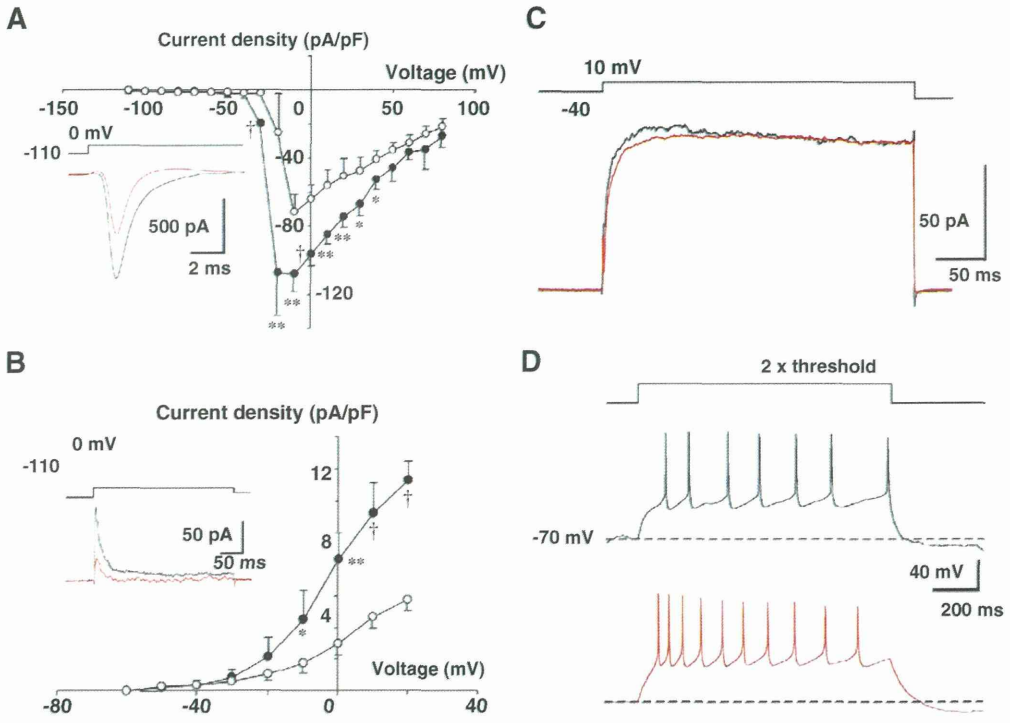

Fig. 4 – Electrophysiological analysis of control and MeCP2-null ES cell-derived neurons. (A) Voltage-dependent Na^+ currents (I_{Na}s) were recorded from control and MeCP2-null ES cell-derived neurons on days 10–12. Current density–voltage (*I–V*) relationships were obtained from control ($n=4$, closed circles) and MeCP2-null neurons ($n=5$, open circles). Inset traces show the mean I_{Na}s elicited by the voltage step pulse from −110 to 0 mV in control (black, $n=4$) and MeCP2-null neurons (red, $n=5$). Symbols for statistical significance: *$P<0.05$; **, $P<0.01$; and †$P<0.001$ (control versus MeCP2-null neurons). (B) Fast inactivating K^+ currents (I_As) were recorded from control and MeCP2-null neurons. *I–V* relationships were obtained from control ($n=4$, closed circles) and MeCP2-null neurons ($n=4$, open circles). Inset traces show the mean I_As elicited by the voltage step pulse from −110 to 0 mV. (C) Sustained K^+ currents (I_{DR}s) were recorded from control (black, $n=3$) and MeCP2-null neurons (red, $n=4$). Each trace shows the mean I_{DR}s elicited by the voltage step pulse from −40 to +10 mV. (D) Response to the depolarizing current pulse injection of membrane was recorded from control (black, $n=6$) and MeCP2-null neurons (red, $n=6$). In each trace, the dashed line indicates the holding membrane potential (−70 mV), and upward deflections during the current pulse injection indicate Na^+ spikes.

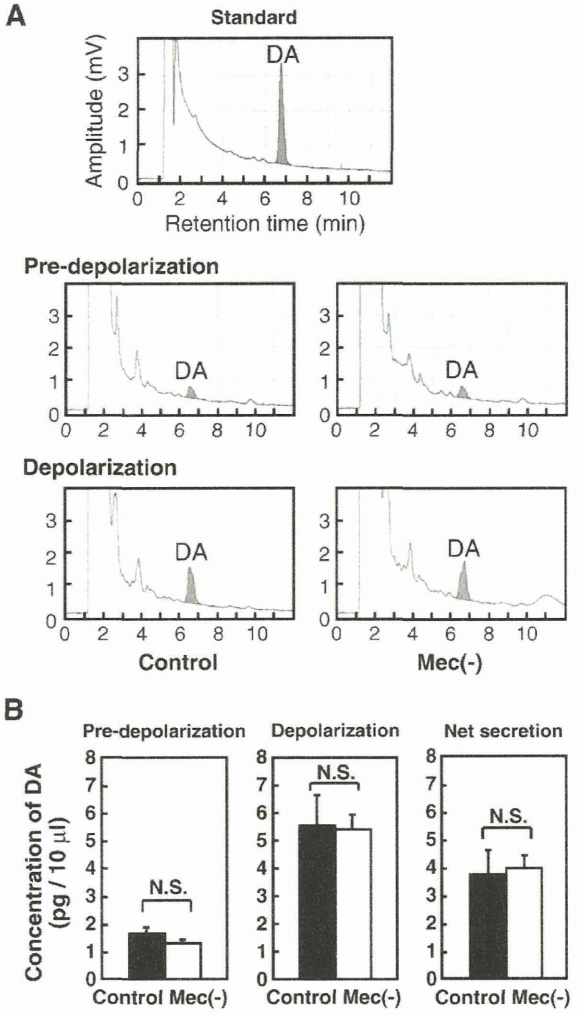

Fig. 5 – Dopamine production and release in MeCP2-null ES cell-derived DNs. (A) Dopamine releases in the media of control and MeCP2-null ES cells on day 10 were analyzed by reverse phase HPLC. The standard panel shows chromatography of a standard solution. DA indicates peaks of dopamine. The retention time for dopamine was 6.5 min in each case. (B) The graphs represent the quantitative HPLC data for dopamine secretion. Dopamine secretion was measured in samples incubated for 15 min with HBSS (pre-depolarization) or high K^+ HBSS (depolarization). Pre-depolarization indicates the spontaneous secretion of dopamine. Net secretion is the depolarized peak release minus the spontaneous dopamine release and shows the response in the presence of potassium. N.S., no significant difference (control versus MeCP2-null ES cells, $n=8$ each).

plasticity in neurons, possibly by stage-specific and neuron-specific methylation of glial genes (Setoguchi et al., 2006).

Interestingly, brain magnetic resonance in MeCP2-null mice demonstrated that metabolism in both neurons and glia was affected (Saywell et al., 2006). In addition, a study using *in vitro* co-culture system has recently demonstrated that MeCP2 mutant astrocytes and their conditioned medium failed to support normal dendritic morphology of hippocampal neurons, suggesting that MeCP2-deficient astrocytes have a non-cell autonomous effect on neuronal properties (Ballas et al., 2009; Maezawa et al., 2009). In general, the coordinated interactions between glia and neurons are crucial for normal neuronal development and function (Allen and Barres, 2009; Corbin et al., 2008; Stevens, 2008). Together with previous data, our results suggest that the main physiological role of MeCP2 in neural development is the inhibition of gliogenesis, and that distorted interactions with abnormally developed glia result in electrophysiologically immature neurons.

Finally, this study may at least in part resolve some of the controversy over whether or not abnormalities in biogenic amine neurotransmitter/receptor systems are associated with RTT (Matsuishi et al., 2001; Temudo et al., 2009; Wenk, 1995). Discrepancies between different studies may be due to the limitations of the experimental strategies, which involved clinical examination of dopamine levels in central spinal fluid, dopamine D2 receptors, or pathological alterations in symptomatic RTT patients (Chiron et al., 1993; Lekman et al., 1990; Perry et al., 1988; Zoghbi et al., 1989, 1985). Here, we demonstrate that MeCP2 is involved in neither the differentiation nor the dopamine production and release of DNs. This has important clinical implications, since whatever abnormalities might exist in the dopaminergic system in RTT patients, they are not directly related to defects in the DNs themselves. However, a potential limitation of the present study is that the ES cell-derived DNs might not be entirely equivalent to DNs in adolescent RTT patients, even though almost all the ES cell colonies were TH-positive. Using this experimental system to uncover the cellular and molecular characteristics of MeCP2-null DNs, in conjunction with studies of MeCP2-null mice and clinical examination of RTT patients, will answer this question definitively in the future.

In conclusion, we have developed an *in vitro* system for analyzing neuronal development and the function of MeCP2. We found that MeCP2 is not essential for maintaining the undifferentiated ES cell state, for neurogenesis, or for DN function; rather, it is mainly involved in inhibiting gliogenesis. Imperfect neuronal maturity, probably resulting from abnormal gliogenesis, may be involved in the pathogenesis of RTT. All the information is useful not only for understanding the developmental roles of MeCP2 and the pathogenesis of RTT, but also for developing therapeutic strategies for RTT in the future.

4. Experimental procedures

4.1. *Recombinant adenoviral vectors*

E1-deleted, replication-deficient adenoviral vector expressing Cre under the transcriptional control of the cytomegalovirus early enhancer and chicken beta-actin promoter (Ad.Cre) or no gene (Ad.dE1.3) was prepared as described previously (Chen et al., 1995; Takahashi et al., 2006).

4.2. *ES cell culture and ACT*

Mouse ES cells in which exons 3 and 4 of Mecp2 were flanked by loxP sites, and which were previously used to generate

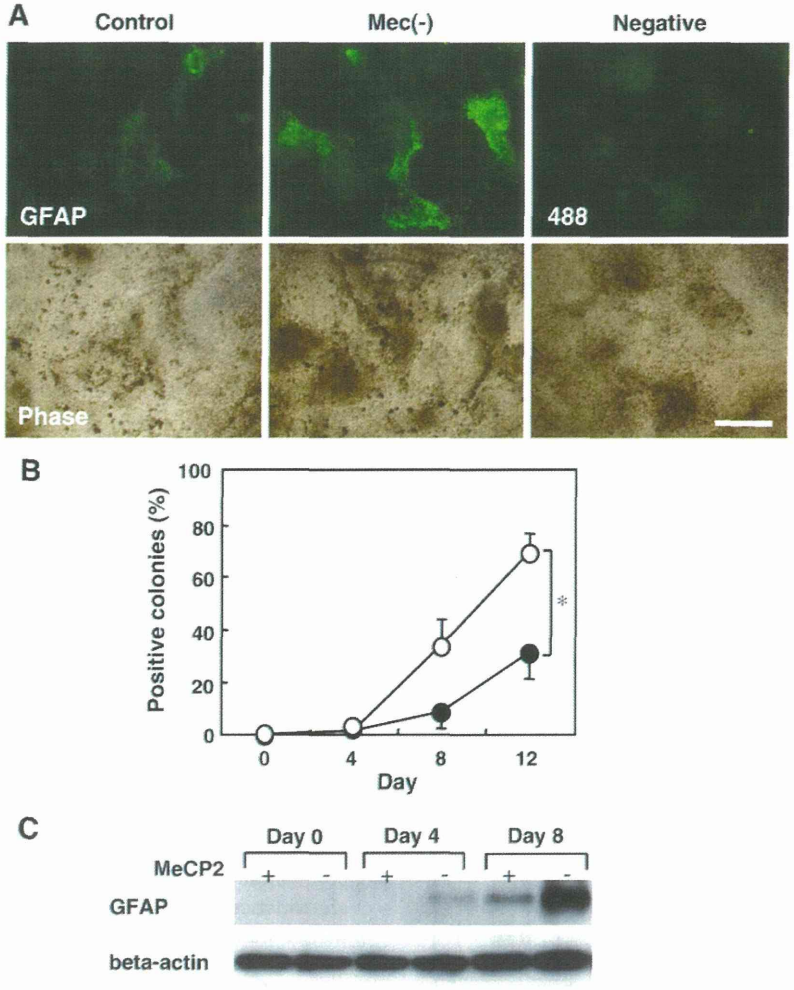

Fig. 6 – Glial differentiation of MeCP2-null ES cells. Control or MeCP2-null ES cell colonies 4, 8, and 12 days after co-culture on PA6 cells were immunostained for GFAP. (A) The top and bottom pictures show immunofluorescent microscopic and phase-contrast observations of ES colonies, respectively, which were stained with an anti-GFAP (green) antibody on day 12. Negative control images show colonies stained with the secondary Alexa Fluor 488 antibody on day 12. Scale bar = 0.5 mm. (B) The graph shows the percentage of control (closed circle) and MeCP2-null (open circle) GFAP-positive ES cell colonies on the indicated days. *$P < 0.05$ (control versus MeCP2-null ES cells, $n = 5$ each, 50–200 colonies per well). Data are means ± SD for three separate measurements from different experiments. (C) Expressions of GFAP protein in control and MeCP2-null ES cells on the indicated days were analyzed by Western blot. Beta-actin protein levels were analyzed in the same way as an internal control.

MeCP2-null mice, were provided by Dr. A. Bird (Guy et al., 2001). ES cells were maintained in the undifferentiated state without feeder cells on gelatin-coated dishes in Glasgow Minimum Essential Medium (G-MEM, GIBCO/BRL, Grand Island, NY, USA) supplemented with 10% fetal bovine serum (FBS), 2 mM L-glutamine (GIBCO/BRL), 1 mM pyruvate (GIBCO/BRL), 0.05 mM 2-mercaptoethanol (2-ME, Nacalai Tesque, Inc., Kyoto, Japan), 0.1 mM nonessential amino acids (GIBCO/BRL), and 2000 U/ml leukemia inhibitory factor (ESGRO, Chemicon International, Temecula, CA) as previously described (Guy et al., 2001; Kawai et al., 2004; Takahashi et al., 2006). MeCP2-null and control ES cells were generated by the ACT method using Ad.Cre and Ad.dE1.3, respectively (Chen et al., 1995; Takahashi et al., 2006). Details are described in the Results section.

Doperminergic neurons were induced essentially as previously described, with some modifications (Kawasaki et al., 2000; Takahashi et al., 2006). Briefly, 1000 MeCP2-null or control ES cells were placed on feeder PA6 cells that had been seeded on collagen-coated eight-well glass plates. Subsequently, these ES cells were co-cultured with PA6 cells in differentiation medium, which consists of G-MEM supplemented 10% knockout serum replacement (KSR, GIBCO/BRL), 2 mM L-glutamine, 1 mM pyruvate, 0.1 mM nonessential amino acids, and 0.1 mM 2-mercaptoethanol as described previously (Kawasaki et al., 2000). The differentiation medium was changed on day 4 and every other day thereafter. After 8 days in differentiation medium, cells were cultured in G-MEM supplemented with N2 (GIBCO/BRL), 100 mM

tetrahydrobiopterin, 200 mM ascorbate, 1 mM pyruvate, 0.1 mM nonessential amino acids, and 0.1 mM 2-mercaptoethanol.

4.3. Animals

The tails of MeCP2-null mice were used as positive controls for genomic PCR (Fig. 1B) in accordance with a protocol approved by the Animal Research Committee of Kurume University and the National Institutes of Health Guidelines for the Care and Use of Laboratory Animals.

4.4. PCR analysis

Genomic DNA was extracted from ES cells and PCR genotyping was performed on genomic DNA using oIMR1436, oIMR1437, and oIMR1438 primers and the protocol provided by the manufacturer (http://jaxmice.jax.org/pub-cgi/protocols/protocols.sh?objtype=protocol&protocol_id=598) (Fig. 1A) (Guy et al., 2001).

Extraction of total RNA, RT-PCR analysis, and electrophoresis were carried out as described previously (Kawai et al., 2004; Takahashi et al., 2006). PCR conditions were as follows: 40 cycles of 94 °C for 30 s, 61 °C for 60 s, and 74 °C for 60 s, using the mouse Mecp2 exon-specific primers 5′-GGTAAAACCCGTCCG GAAAATG-3′ (sense) and 5′-TTCAGTGGCTTGTCTCTGAG-3′ (antisense) (Kriaucionis and Bird, 2004).

4.5. Immunocytochemistry

Cells were stained using antibodies against Nestin (dilution 1:100, clone 25, BD Biosciences Pharmingen, San Diego, CA), Tyrosine hydroxylase (TH) (dilution 1:100, clone AB152, Chemicon International), β-Tubulin type III (dilution 1:500, TuJ, Sigma-Aldrich, Inc., St. Louis, MO), GFAP (dilution 1:500, clone G-A-5, Sigma-Aldrich, Inc.), Oct-4 (dilution 1:500, clone C-10, Santa Cruz Biotechnology, Inc., Santa Cruz, CA), or Stat-3 (dilution 1:500, C-20, Santa Cruz Biotechnology, Inc.), together with secondary fluorescent antibodies (dilution 1:500) as described previously (Kawai et al., 2004; Takahashi et al., 2006). As a negative control, cells were stained with only secondary fluorescent antibodies without primary antibodies (Figs. 3, 6A, and Suppl. Fig. 1).

4.6. Immunoblotting

Protein was extracted from ES cells and Western blot analysis was performed using anti-GFAP (clone G-A-5) and anti-Actin (clone AC-40, Sigma-Aldrich, Inc.) monoclonal antibodies, and detected with horseradish peroxidase-conjugated anti-mouse IgG (DakoCytomation, Glostrup, Denmark) and chemiluminescent substrate (Chemi-Lumi One, Nacalai Tesque, Inc.), as described previously (Takahashi et al., 2006).

4.7. Electrophysiological analysis

Electrophysiological measurements were performed as described previously (Murai and Akaike, 2005). Briefly, whole cell patch-clamp recordings were made from 29 ES cell-derived neurons with glass patch-pipettes. The resistance of patch electrodes was 4–8 MΩ. Cells were voltage or current clamped. The membrane currents or potentials were measured with a patch-clamp amplifier (Axopatch 200A, Axon Instruments Inc., Union City, CA, USA). Whole cell currents or membrane potentials were low-pass filtered at 1–2 kHz, digitized at a sampling rate of 20 kHz, and stored on a computer hard disc (pCLAMP 8, Axon Instruments Inc.). Series resistance was compensated by 50–70%. All experiments were performed at room temperature (21–24 °C).

The membrane was first held at −110 mV and then depolarized by voltage step pulses (300 ms duration) from −110 to +80 mV with 10 mV steps to elicit the membrane currents. In the absence and presence of voltage-dependent Na^+ channel blocker, tetrodotoxin (TTX, 300 nM), the total membrane currents and TTX resistant (TTX-R) currents were obtained, respectively. The voltage-dependent sodium (Na^+) current, which is TTX sensitive (TTX-S), was obtained by subtracting the TTX-R currents from the total membrane currents in both the control and MeCP2-null ES cell-derived neurons.

Two types of voltage-dependent potassium (K^+) currents were also recorded in both the control and the MeCP2-null ES cell-derived neurons: fast inactivating K^+ current (A-type K^+ current, I_A) and sustained K^+ current (delayed rectifier K^+ current, I_{DR}), sensitive to 4-aminopyridine (4-AP, 1 mM) and tetraethylammonium-chloride (TEA-Cl, 20 mM), respectively. The voltage step pulse from −110 to +20 mV with 10 mV step (300 ms duration) in the presence of TTX (300 nM) elicited the combined membrane K^+ currents. To obtain I_{DR}, the membrane was first held at −40 mV and then depolarized from −40 to +20 mV with 10 mV steps (300 ms duration), because I_A inactivated at −40 mV and I_{DR} was activated from −40 mV. Subtraction of I_{DR} from the combined membrane K^+ currents yielded I_A.

In current-clamp recording, injection of the depolarizing current pulse (2 ms, 0.15–0.20 nA) elicited an action potential just after the end of the current injection. In both control and MeCP2-null ES cell-derived neurons, injection of a prolonged depolarizing current pulse (1 s duration and two times the intensity for the threshold) elicited repetitive firings during membrane depolarization.

4.8. High performance liquid chromatography (HPLC)

To measure dopamine content and secretion in MeCP2-null and control ES cells that were differentiated into DNs on PA6 cells for 10 days, an HPLC electrochemical detector (ECD) system (HTEC-500, Eicom Corp., Kyoto, Japan) was used in accordance with the manufacturer's protocol, with some modifications (Kawasaki et al., 2000). Briefly, ES cells cultured in six-well plates were washed twice with Hanks' balanced salt solution (HBSS), then incubated for 15 min in high K^+ (56 mM) HBSS to evoke membrane depolarization. The incubation buffer (a 500 ml aliquot) was collected and centrifuged at 800×*g* for 10 min to remove detached cells, and the 400 ml supernatant was mixed with 400 ml of 20 mM hydrochloric acid and 100 mM EDTA. Ten microliters of each sample was injected into the HPLC-ECD system and separated with a reverse phase column (Eicompak CA-50DS, Eicom) using 0.1 M phosphate buffer (pH 6.0) containing 2.3 mM 1-octanesulfonic acid, 0.13 mM EDTA, and 20% methanol as a

mobile phase at a flow rate of 0.23 ml/min. The retention time for dopamine was 6–8 min. The amount of dopamine in each sample was calculated by using the peak height ratio relative to the standard dopamine hydrochloride (H8502, Sigma-Aldrich, Inc.) solution.

4.9. *Statistical analysis*

Quantitative results are expressed as means±SD. The Student's *t*-test was used to compare data, with $p<0.05$ considered significant.

Supplementary materials related to this article can be found online at doi:10.1016/j.brainres.2010.08.090.

Competing interests statement

The authors declare that they have no competing financial interests.

Acknowledgments

This work was supported in part by a project for establishing open research centers in private universities, a Grant-in-Aid for Scientific Research (B) and a Grant-in-Aid for Young Scientists (B) from the Japan Society for the Promotion of Science, and by a Grant from Terumo Life Science Foundation. We would like to thank Adrian Bird for providing the MeCP2 targeted ES cells; and Kaori Noguchi, Chikako Goto, and Aya Niihara for technical assistance.

REFERENCES

Allen, N.J., Barres, B.A., 2009. Neuroscience: Glia—more than just brain glue. Nature 457, 675–677.

Amir, R.E., Van den Veyver, I.B., Wan, M., Tran, C.Q., Francke, U., Zoghbi, H.Y., 1999. Rett syndrome is caused by mutations in X-linked MECP2, encoding methyl-CpG-binding protein 2. Nat. Genet. 23, 185–188.

Armstrong, D.D., 2002. Neuropathology of Rett syndrome. Ment. Retard. Dev. Disabil. Res. Rev. 8, 72–76.

Ballas, N., Lioy, D.T., Grunseich, C., Mandel, G., 2009. Non-cell autonomous influence of MeCP2-deficient glia on neuronal dendritic morphology. Nat. Neurosci. 12, 311–317.

Biella, G., Di Febo, F., Goffredo, D., Moiana, A., Taglietti, V., Conti, L., Cattaneo, E., Toselli, M., 2007. Differentiating embryonic stem-derived neural stem cells show a maturation-dependent pattern of voltage-gated sodium current expression and graded action potentials. Neuroscience 149, 38–52.

Bienvenu, T., Chelly, J., 2006. Molecular genetics of Rett syndrome: when DNA methylation goes unrecognized. Nat. Rev. Genet. 7, 415–426.

Chahrour, M., Zoghbi, H.Y., 2007. The story of Rett syndrome: from clinic to neurobiology. Neuron 56, 422–437.

Chahrour, M., Jung, S.Y., Shaw, C., Zhou, X., Wong, S.T., Qin, J., Zoghbi, H.Y., 2008. MeCP2, a key contributor to neurological disease, activates and represses transcription. Science 320, 1224–1229.

Chen, R.Z., Akbarian, S., Tudor, M., Jaenisch, R., 2001. Deficiency of methyl-CpG binding protein-2 in CNS neurons results in a Rett-like phenotype in mice. Nat. Genet. 27, 327–331.

Chen, S.H., Chen, X.H., Wang, Y., Kosai, K., Finegold, M.J., Rich, S.S., Woo, S.L., 1995. Combination gene therapy for liver metastasis of colon carcinoma in vivo. Proc. Natl. Acad. Sci. U. S. A. 92, 2577–2581.

Chiron, C., Bulteau, C., Loc'h, C., Raynaud, C., Garreau, B., Syrota, A., Maziere, B., 1993. Dopaminergic D2 receptor SPECT imaging in Rett syndrome: increase of specific binding in striatum. J. Nucl. Med. 34, 1717–1721.

Corbin, J.G., Gaiano, N., Juliano, S.L., Poluch, S., Stancik, E., Haydar, T.F., 2008. Regulation of neural progenitor cell development in the nervous system. J. Neurochem. 106, 2272–2287.

Deguchi, K., Antalffy, B.A., Twohill, L.J., Chakraborty, S., Glaze, D.G., Armstrong, D.D., 2000. Substance P immunoreactivity in Rett syndrome. Pediatr. Neurol. 22, 259–266.

Ficker, E., Heinemann, U., 1992. Slow and fast transient potassium currents in cultured rat hippocampal cells. J. Physiol. 445, 431–455.

Guy, J., Hendrich, B., Holmes, M., Martin, J.E., Bird, A., 2001. A mouse Mecp2-null mutation causes neurological symptoms that mimic Rett syndrome. Nat. Genet. 27, 322–326.

Ide, S., Itoh, M., Goto, Y., 2005. Defect in normal developmental increase of the brain biogenic amine concentrations in the mecp2-null mouse. Neurosci. Lett. 386, 14–17.

Jellinger, K.A., 2003. Rett syndrome—an update. J. Neural Transm. 110, 681–701.

Kawai, T., Takahashi, T., Esaki, M., Ushikoshi, H., Nagano, S., Fujiwara, H., Kosai, K., 2004. Efficient cardiomyogenic differentiation of embryonic stem cell by fibroblast growth factor 2 and bone morphogenetic protein 2. Circ. J. 68, 691–702.

Kawasaki, H., Mizuseki, K., Nishikawa, S., Kaneko, S., Kuwana, Y., Nakanishi, S., Nishikawa, S.I., Sasai, Y., 2000. Induction of midbrain dopaminergic neurons from ES cells by stromal cell-derived inducing activity. Neuron 28, 31–40.

Kishi, N., Macklis, J.D., 2004. MECP2 is progressively expressed in post-migratory neurons and is involved in neuronal maturation rather than cell fate decisions. Mol. Cell. Neurosci. 27, 306–321.

Kriaucionis, S., Bird, A., 2004. The major form of MeCP2 has a novel N-terminus generated by alternative splicing. Nucleic Acids Res. 32, 1818–1823.

Lekman, A., Witt-Engerstrom, I., Holmberg, B., Percy, A., Svennerholm, L., Hagberg, B., 1990. CSF and urine biogenic amine metabolites in Rett syndrome. Clin. Genet. 37, 173–178.

Maezawa, I., Swanberg, S., Harvey, D., LaSalle, J.M., Jin, L.W., 2009. Rett syndrome astrocytes are abnormal and spread MeCP2 deficiency through gap junctions. J. Neurosci. 29, 5051–5061.

Matsuishi, T., Yamashita, Y., Kusaga, A., 2001. Neurobiology and neurochemistry of Rett syndrome. Brain Dev. 23 (Suppl 1), S58–S61.

Mnatzakanian, G.N., Lohi, H., Munteanu, I., Alfred, S.E., Yamada, T., MacLeod, P.J., Jones, J.R., Scherer, S.W., Schanen, N.C., Friez, M.J., Vincent, J.B., Minassian, B.A., 2004. A previously unidentified MECP2 open reading frame defines a new protein isoform relevant to Rett syndrome. Nat. Genet. 36, 339–341.

Murai, Y., Akaike, T., 2005. Orexins cause depolarization via nonselective cationic and K+ channels in isolated locus coeruleus neurons. Neurosci. Res. 51, 55–65.

Nagai, K., Miyake, K., Kubota, T., 2005. A transcriptional repressor MeCP2 causing Rett syndrome is expressed in embryonic non-neuronal cells and controls their growth. Brain Res. Dev. Brain Res. 157, 103–106.

Perry, T.L., Dunn, H.G., Ho, H.H., Crichton, J.U., 1988. Cerebrospinal fluid values for monoamine metabolites, gamma-aminobutyric acid, and other amino compounds in Rett syndrome. J. Pediatr. 112, 234–238.

Qian, X., Shen, Q., Goderie, S.K., He, W., Capela, A., Davis, A.A., Temple, S., 2000. Timing of CNS cell generation: a programmed sequence of neuron and glial cell production from isolated murine cortical stem cells. Neuron 28, 69–80.

Samaco, R.C., Mandel-Brehm, C., Chao, H.T., Ward, C.S., Fyffe-Maricich, S.L., Ren, J., Hyland, K., Thaller, C., Maricich, S.M., Humphreys, P., Greer, J.J., Percy, A., Glaze, D.G., Zoghbi, H.Y., Neul, J.L., 2009. Loss of MeCP2 in aminergic neurons causes cell-autonomous defects in neurotransmitter synthesis and specific behavioral abnormalities. Proc. Natl. Acad. Sci. U. S. A. 106, 21966–21971.

Saywell, V., Viola, A., Confort-Gouny, S., Le Fur, Y., Villard, L., Cozzone, P.J., 2006. Brain magnetic resonance study of Mecp2 deletion effects on anatomy and metabolism. Biochem. Biophys. Res. Commun. 340, 776–783.

Setoguchi, H., Namihira, M., Kohyama, J., Asano, H., Sanosaka, T., Nakashima, K., 2006. Methyl-CpG binding proteins are involved in restricting differentiation plasticity in neurons. J. Neurosci. Res. 84, 969–979.

Shahbazian, M.D., Antalffy, B., Armstrong, D.L., Zoghbi, H.Y., 2002. Insight into Rett syndrome: MeCP2 levels display tissue- and cell-specific differences and correlate with neuronal maturation. Hum. Mol. Genet. 11, 115–124.

Smrt, R.D., Eaves-Egenes, J., Barkho, B.Z., Santistevan, N.J., Zhao, C., Aimone, J.B., Gage, F.H., Zhao, X., 2007. Mecp2 deficiency leads to delayed maturation and altered gene expression in hippocampal neurons. Neurobiol. Dis. 27, 77–89.

Stevens, B., 2008. Neuron-astrocyte signaling in the development and plasticity of neural circuits. Neurosignals 16, 278–288.

Takahashi, T., Kawai, T., Ushikoshi, H., Nagano, S., Oshika, H., Inoue, M., Kunisada, T., Takemura, G., Fujiwara, H., Kosai, K., 2006. Identification and isolation of embryonic stem cell-derived target cells by adenoviral conditional targeting. Mol. Ther. 14, 673–683.

Temudo, T., Rios, M., Prior, C., Carrilho, I., Santos, M., Maciel, P., Sequeiros, J., Fonseca, M., Monteiro, J., Cabral, P., Vieira, J.P., Ormazabal, A., Artuch, R., 2009. Evaluation of CSF neurotransmitters and folate in 25 patients with Rett disorder and effects of treatment. Brain Dev. 31, 46–51.

Tsujimura, K., Abematsu, M., Kohyama, J., Namihira, M., Nakashima, K., 2009. Neuronal differentiation of neural precursor cells is promoted by the methyl-CpG-binding protein MeCP2. Exp. Neurol. 219, 104–111.

Wenk, G.L., 1995. Alterations in dopaminergic function in Rett syndrome. Neuropediatrics 26, 123–125.

Zoghbi, H.Y., Percy, A.K., Glaze, D.G., Butler, I.J., Riccardi, V.M., 1985. Reduction of biogenic amine levels in the Rett syndrome. N. Engl. J. Med. 313, 921–924.

Zoghbi, H.Y., Milstien, S., Butler, I.J., Smith, E.O., Kaufman, S., Glaze, D.G., Percy, A.K., 1989. Cerebrospinal fluid biogenic amines and biopterin in Rett syndrome. Ann. Neurol. 25, 56–60.

The American Journal of Pathology, Vol. 176, No. 2, February 2010

DOI: 10.2353/ajpath.2010.090222

Cell Injury, Repair, Aging and Apoptosis

Anti-Fas Gene Therapy Prevents Doxorubicin-Induced Acute Cardiotoxicity through Mechanisms Independent of Apoptosis

Shusaku Miyata,* Genzou Takemura,* Ken-ichiro Kosai,† Tomoyuki Takahashi,‡ Masayasu Esaki,* Longhu Li,* Hiromitsu Kanamori,* Rumi Maruyama,* Kazuko Goto,* Akiko Tsujimoto,* Toshiaki Takeyama,* Tomonori Kawaguchi,* Takamasa Ohno,§ Kazuhiko Nishigaki,* Takako Fujiwara,¶ Hisayoshi Fujiwara,* and Shinya Minatoguchi*

From the Division of Cardiology, Gifu University Graduate School of Medicine, Gifu; the Department of Gene Therapy and Regenerative Medicine,† Kagoshima University Graduate School of Medicine and Dental Sciences, Kagoshima; the Division of Gene Therapy and Regenerative Medicine,‡ Cognitive and Molecular Research Institute of Brain Diseases, Kurume University, Kurume; the Laboratory of Medical Resources,§ School of Pharmacy, Aichi Gakuin University, Nagoya; and the Department of Food Science,¶ Kyoto Women's University, Kyoto, Japan*

Activation of Fas signaling is a key mediator of doxorubicin cardiotoxicity, which involves both cardiomyocyte apoptosis and myocardial inflammation. In this study, acute cardiotoxicity was induced in mice by doxorubicin, and some mice simultaneously received an intramuscular injection of adenoviral vector encoding mouse soluble Fas (sFas) gene (Ad.CAG-sFas), an inhibitor of Fas/Fas ligand interaction. Two weeks later, left ventricular dilatation and dysfunction were apparent in the LacZ-treated control group, but both were significantly mitigated in the sFas-treated group. The *in situ* nick-end labeling-positive rate were similar in the two groups, and although electron microscopy revealed cardiomyocyte degeneration, no apoptotic structural features and no activation of caspases were detected, suggesting an insignificant role of apoptosis in this model. Instead, sFas treatment reversed doxorubicin-induced down-regulation of GATA-4 and attenuated ubiquitination of myosin heavy chain and troponin I to preserve these sarcomeric proteins. In addition, doxorubicin-induced significant leukocyte infiltration, fibrosis, and oxidative damage to the myocardium, all of which were largely reversed by sFas treatment. sFas treatment also suppressed doxorubicin-induced p53 overexpression, phosphorylation of c-Jun N-terminal kinase, c-Jun, and inhibitor of nuclear factor-κB, as well as production of cyclooxygenase-2 and monocyte chemoattractant protein-1, and it restored extracellular signal-regulated kinase activation. Therefore, sFas gene therapy prevents the progression of doxorubicin-induced acute cardiotoxicity, with accompanying attenuation of the cardiomyocyte degeneration, inflammation, fibrosis, and oxidative damage caused by Fas signaling. ***(Am J Pathol 2010, 176:687–698; DOI: 10.2353/ajpath.2010.090222)***

The antineoplastic drug doxorubicin (adriamycin) is effective in the treatment of a broad range of hematogenous and solid human malignancies, but its clinical use is limited by its dose-dependent side effects: irreversible degenerative cardiomyopathy and congestive heart failure.[1–3] The efficacy of doxorubicin against cancer has prompted a search to find treatments that reduce or prevent its cardiac side effects.[3,4] So far, however, the ability of these treatments to protect the heart from doxorubicin has been varied and limited.

The interaction of Fas with Fas ligand is an important trigger for apoptosis in many cell types, particularly cells related to the immune system.[5] Moreover, it has recently come to light that the Fas/Fas ligand interaction plays an important role in the development and progression of doxorubicin cardiomyopathy. Nakamura et al showed that in a rat doxorubicin cardiomyopathy model, myocardial Fas expression and cardiomyocyte apoptosis were concomitantly increased and that a neutralizing antibody against Fas ligand attenuated both, leading to improvement in cardiac function.[6] In addition, Yamaoka et al

Supported in part by grants-in-aid for scientific research 15209027, 15590732, 14570700, and 13470143 from the Ministry of Education, Science and Culture of Japan.

Accepted for publication October 21, 2009.

Address reprint requests to Genzou Takemura, M.D., Ph.D., Division of Cardiology, Gifu University Graduate School of Medicine, 1-1 Yanagido, Gifu 501-1194, Japan. E-mail: gt@gifu-u.ac.jp.